EXPERIMENTAL OBSERVATIONS OF THE DYNAMICS OF WAKES OF MAGNETIC OBSTACLES

DOMÍNGUEZ[1] D.R., ROMÁN[1] J.J., BELTRÁN[2] A., CUEVAS[1] S. and RAMOS[1] E.
[1] Renewable Energy Institute, Universidad Nacional Autónoma de México, 62580, Temixco Mor. Mexico,
[2] Materials Research Institute, Universidad Nacional Autónoma de México, 04510, México D.F., Mexico.
E-mail address of corresponding author: erm@ier.unam.mx

Abstract: Experimental recordings of the flow generated by magnetic obstacles have been made using a liquid metal flowing through a localized magnetic field. The relative motion of the fluid and the magnetic field generate electric currents that in turn produce a Lorentz force that opposes the motion of the fluid at the position where the magnetic field is located. This effect is known as a magnetic obstacle. Previous theoretical studies predict that for a given Hartmann number, the flow transits from a steady state to a time-dependent state as the Reynolds number grows. If the Reynolds number is increased further, the flow becomes steady again. Our experimental observations suggest that this prediction is correct.

1. Introduction

A magnetic obstacle is defined as the force that opposes the flow of an electricity conducting fluid due to the presence of a localized magnetic field. The relative motion between the fluid and the applied magnetic field induces electric currents that in turn generate a magnetic field and a Lorentz force that tends to disturb the original flow. This phenomenon was identified in the 70's [1], [2] and has been analyzed more recently in references [3] - [8]. The flow topology and stability has been described in terms of the Reynolds (Re) and Hartmann (Ha) numbers both from the experimental and numerical view points. An important feature of the wakes generated by magnetic obstacles, detected with the ultrasonic velocity profile method, is that the length of the recirculation region behind the magnetic obstacle increases with the Reynolds number to reach a maximum and then decreases [7]. Theoretical studies indicate that the for large enough Hartmann numbers, increasing the Reynolds number results in the formation of a wake behind the magnetic obstacle with characteristics similar to a von Kármán vortex street that occurs behind a rigid obstacle, but in sharp contrast to this last case, a further increase of the Reynolds number leads to a reduction of vortex shedding behind the magnetic obstacle [8]. In the present contribution, we describe the experimental recordings that were made to detect the axial velocity of the flow of a liquid metal in presence of a magnetic obstacle with the objective of determining representative properties of the wake that allow us to infer the dynamics of the whole structure of the wake.

2. Experimental setup

The experimental device used in the observations described in this report is a rectangular loop made of acrylic (Polymethyl methacrylate) walls with a rectangular effective cross section of 1 cm x 8 cm. The lengths of the large and short legs of the duct are 85.8 cm and 40 cm respectively. The loop is built in sections joined with flanges and the whole system is fixed with mounts that separate it from the floor of the table, making it easier to detect possible leaks. Straddling at the central region of one of the long legs a rotatory MHD pump is located. The pump consists of a motor that spins two disks where 24 permanent magnets are mounted radially. This device sets the liquid metal in motion around the loop. A photograph of the liquid metal loop is shown in Figure 1.

Figure 1: The experimental liquid metal loop. The MHD pump is in the far long leg. The disk and the liquid metal rotate in the counterclockwise direction. The magnet is near the middle of the near long leg, 30 cm away from the upstream corner and 4 cm over the lower wall of the duct. The ultrasonic gauge is in the far right of the picture.

The working fluid is a Ga(68%) In(20%)Sn(12%) eutectic mixture which has a melting temperature of 10.5 oC. The magnetic obstacle is created with two 2.54 x 2.54 x 1.25 cm Neodynium magnets placed on the outer side of opposite vertical walls of the central part of one of the long legs. The magnets are located at 30 cm from the upstream corner and 4 cm from the lower horizontal wall of the duct. With this magnet arrangement, the maximum magnetic field that can be obtained at the center of the duct is 0.23 T. The position of the magnets is illustrated in Figure 1. The velocity of the liquid metal is measured with a Signal Processing ultrasonic Doppler velocimeter (UDV) using a probe 0.8 cm in diameter and a wave frequency of 4 Hz. With this equipment it is possible to determine one component of the velocity along the propagation line of acoustic wave emerging from the emitter. The ultrasonic gauge was fixed at the downstream end of the region of analysis to detect the axial velocity along the axial coordinate. An appropriate mount was used to place the gauge different vertical positions. In steady-state flows, axial measurements at different vertical positions allow the reconstruction of the axial velocity distribution in the vertical plane. Given that the geometry of the duct and the physical properties of the fluid are fixed, the range of Reynolds numbers available in the experimental equipment depends on the power delivered by the pump (or equivalently the pressure difference) and the resistance of the duct. The most accurate way to estimate the Reynolds number is through direct calibration. This is done by detecting the distribution of the average axial velocity in absence of magnetic field for a range of MHD pump rotation rates. Once this variable is measured the Reynolds based on the hydraulic diameter of the cross section can be calculated and for our experimental conditions it is $869 < Re < 4960$. The range of Hartmann numbers available depends on the intensity of the permanent magnets used and their relative position with respect to the liquid metal. Increasing the distance of the magnets to the vertical walls reduces the effective magnitude of the magnetic field inside the duct and a range of Hartmann numbers can be obtained. Under the geometry of our experiment, and for the liquid metal used, we have $57 < Ha < 96$.

3. Theoretical remarks

A theoretical model for a quasi two-dimensional MHD flow in presence of a magnetic obstacle reported previously has been used in the interpretation of the experimental recordings; here we describe only the salient features. More details are given in reference [8].

The model consists on the mass and momentum conservation equations including the Lorentz force as a source of momentum of the form

$$\mathbf{S} = \frac{Ha^2}{Re}\mathbf{j} \times \mathbf{B_o}, \qquad (1)$$

where **j** is the electric current, and **Bo** is the externally imposed magnetic field which has a localized spatial distribution corresponding to a pair of permanent magnets of small dimensions compared with the test section of the duct. The electric current is calculated using the equation for the induced magnetic field in the direction perpendicular to the vertical planes and Ampere's law. The non-dimensional parameters are the Reynolds and the Hartmann numbers defined by

$$Re = \frac{UL}{\nu} \quad \text{and} \quad Ha = B_o D\sqrt{\frac{\sigma}{\rho\nu}} \qquad (2)$$

In the previous equations, *L* is the hydraulic diameter of the duct and *D* is the gap between the vertical walls of the duct. The symbol *U* is the vertical average axial velocity and ν, ρ, and σ stand for the kinematic viscosity, the density and the electric conductivity respectively.
The boundary conditions considered are uniform flow at the channel entrance and outflow at the downstream end of the integration volume. At the lateral walls, periodic boundary conditions are considered.
Theoretical results found in reference [8] indicate that for a given Hartmann number, and small Reynolds numbers, no vortices are shed. For a Reynolds number larger than a threshold which depends on the Hartmann number, vortices are shed but only for a Reynolds number interval, ie., for a given Hartmann number, vortex shedding is suppressed for large enough Reynolds numbers. As is described below, this feature is consistent with the observed in the experimental records reported.

4. Experimental results

In all results reported, the axis of coordinates is defined at the center of the magnet with the axial and transversal coordinates increasing in the downstream and upward directions respectively. The axial velocity u_x in the (x, t) space as obtained with the UDV is plotted according to the color code bar for Ha = 96 and Re =2965 and for the vertical position y = -12.7 mm. The left panel displays the velocity $u_x(x; t)$ for 0< t< 100 s. and the right panel is a zoom to show the detail. The most salient feature of the records is that the axial velocity just upstream of the magnet is reduced and then it grows in the region 0< x < 100 mm. as compared with its upstream value. The inclined, parallel strips recorded in the region x > 200 mm indicate the transit of a periodic perturbation in time for a fixed point in space, or in space for a snapshot.

In order to a make a quantitative analysis, we show in Figure 3 a sample of velocity at the fixed point (x = 250 mm, y = -12.7 mm) as a function of time for Ha = 60 and Re = 869, 2965, 4520 and 4960. The original traces have been smoothed with a moving average filter of 15 points.
The intensity of the flow can be quantified in terms of the parameter $\mathcal{A}$ related to the amplitude of the oscillation as

$$\mathcal{A} = u_x - < u_x > \qquad (3)$$

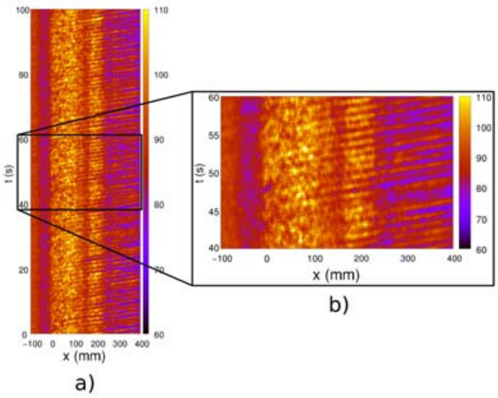

Figure 2: Map of axial velocity u_x in the (x,t) space, y = -12.7 mm. The panel on the right hand side is a zoom. The color indicates the magnitude of the axial velocity. Re = 2965, Ha = 96.

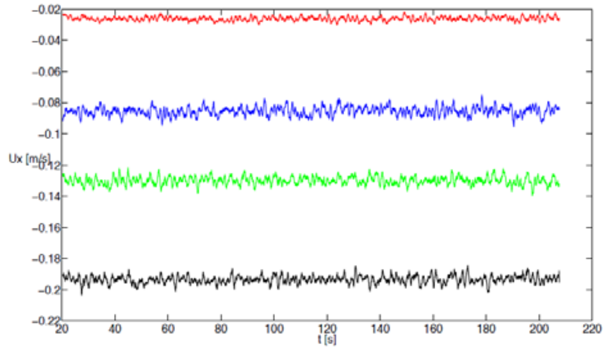

Figure 3: Axial velocity u_x as a function of time at the point x = 250 mm, y = -12.7 mm for Ha = 60. Starting from the top, traces were obtained for Re= 869, 2965, 4520 and 4960.

where $< u_x >$ is the average axial velocity over a time interval I. In Fig. 4 we show an example of the parameter $\mathcal{A}$ as a function of time for three Reynolds numbers, Re=869, 2965 and 4960. Although the dynamic behavior of the traces is complex, inspection indicates that the amplitude of the traces is not a monotonous function of the Reynolds number. In order to make a more quantitative assertion, we also define the parameter $\mathcal{L}2$ as:

$$\mathcal{L}^2 = \frac{1}{I}\int_o^I \mathcal{A}^2 dt \qquad (4)$$

Notice that $\mathcal{L}2$ is a function of the Hartmann and Reynolds numbers only and indicates the average of the square of the amplitude of the axial velocity oscillation with respect to its average value in the interval I.

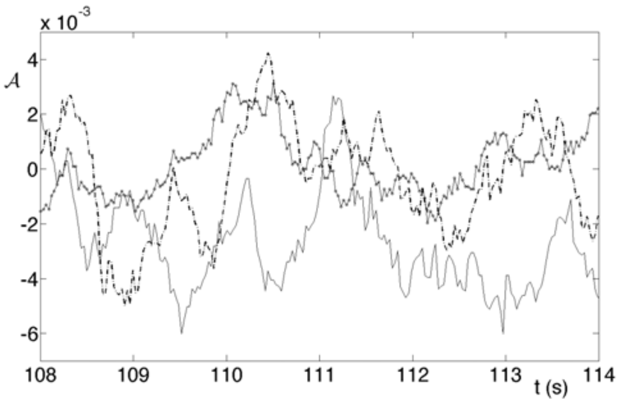

Figure 4: The parameter $\mathcal{A}$ as a function of time for three Reynolds numbers: Re = 869 (line-circles), 2965 (line) and 4960(line-dot).

In figure 5, $\mathcal{L}2$ is shown as a function of Re for Hartmann = 60. As it can be appreciated, for Re < Re_M= 4033 the trace is an increasing function of Reynolds number, but then, it reaches a maximum to decrease for larger Reynolds numbers. This experimental record is consistent with the theoretical result which indicates that after a critical Reynolds number, the vortices in the wake of the magnetic obstacle reduce their intensity as the Reynolds number increases.

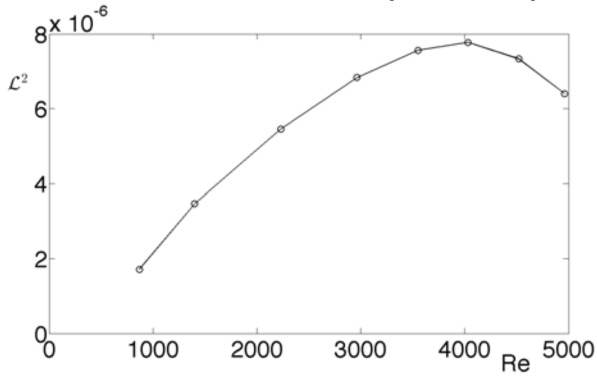

Figure 5: The parameter $\mathcal{L}2$ as a function of the Reynolds number for Ha = 60. The trace of $\mathcal{L}2$ attains a maximum at ReM = 4033.

5. Conclusion

Experimental records of the wake formed by a magnetic obstacle in a liquid metal made with an ultrasonic velocimeter have been presented. The velocity records show the presence of intermittent perturbations that indicate the presence of vortex shedding. In the magnetic obstacle, where a local body force opposes the flow, for flows with a Reynolds number larger that a critical value (Re ~ 4000), we observe that increasing the Reynolds number reduces the oscillatory motion in the wake, reducing in turn the influence of the presence of the obstacle in the downstream flow. This observation is in agreement with a Q2D theory reported previously.

6. References

[1] Gelfgat, Y. M. and Olshanskii, S. V. Velocity structure of flows in non-uniform constant magnetic fields. ii. experimental results. Magnetohydrodynamics **14**, 151–154 (1978)

[2] Gelfgat, Y. M., Peterson, D. E. and Shcherbinin, E. V. Velocity structure of flows in nonuniform constant magnetic fields 1. Numerical calculations. Magnetohydrodynamics **14**, 55–61 (1978)

[3] Cuevas, S.; Smolentsev, S. and Abdou, M. A.: On the flow past a magnetic obstacle. J. Fluid. Mech. **553**, 227-252 (2006)

[4] Cuevas, S.; Smolentsev, S. and Abdou, M. A.: Vorticity generation in the creeping flow past a magnetic obstacle. Phys. Rev E **74** 056301 (2006)

[5] Votyakov E. V., Kolesnikov Y. Andreev O., Zienicke E. and Thess A.: Structure of the wake of a magnetic obstacle. Phys. Rev. Lett. **98**, 144504 (2007)

[6] Votyakov E. V., Zienicke E. and Kolesnikov Y. B. Constrained flow around a magnetic obstacle. J. Fluid Mech. **610**, 131- 156 (2008)

[7] Andreev O., Kolesnikov Y. and Thess A. Application of the ultrasonic velocity profile method to the mapping of liquid metal flows under the influence of a non-uniform magnetic field. Exp. Fluids **49,** 77-83, (2009)

[8] Ramos E., Beltrán A. Cuevas S. and Smolentsev S.: Dynamic properties of a magnetic obstacle. Fundamental and Applied MHD, Book of abstracts, 7th International PAMIR conference, Volume 2, pp 891-895. Presqu'Ile de Giens, France (2008)